Global transcriptome analysis of *Aedes aegypti* mosquitoes in response to Zika virus infection

Kayvan Etebari[1], Shivanand Hegde[2], Miguel A Saldaña[3], Steven G Widen[4], Thomas G Wood[4], Sassan Asgari[1#], Grant L Hughes[5#].

[1]Australian Infectious Disease Research Centre, School of Biological Sciences, The University of Queensland, Brisbane, Australia

[2]Department of Pathology, University of Texas Medical Branch, Galveston, TX, USA

[3]Department of Microbiology and Immunology, University of Texas Medical Branch, Galveston, TX, USA

[4]Department of Biochemistry and Molecular Biology, University of Texas Medical Branch, Galveston, TX, USA

[5]Department of Pathology, Institute for Human Infections and Immunity, Center for Tropical Diseases, Center for Biodefense and Emerging Infectious Disease. University of Texas Medical Branch, Galveston, TX, USA

Word counts: Abstract+Importance (327); text (4196)

Running title: Transcriptional changes to Zika virus in mosquitoes

[#]Corresponding authors: Sassan Asgari – s.asgari@uq.edu.edu. Grant L Hughes glhughes@utmb.edu.

Abstract

Zika virus (ZIKV) of the *Flaviviridae* family is a recently emerged mosquito-borne virus that has been implicated in the surge of the number of microcephaly instances in south America. The recent rapid spread of the virus led to its declaration as a global health emergency by the World Health Organization. The virus is transmitted mainly by the mosquito *Aedes aegypti* that also vectors dengue virus, however little is known about the interactions of the virus with the mosquito vector. In this study, we investigated the transcriptome profiles of whole *Ae. aegypti* mosquitoes in response to ZIKV infection at 2, 7, and 14 days post-infection using RNA-Seq. Results showed changes in the abundance of a large number of transcripts at each time point following infection, with 18 transcripts commonly changed among the three time points. Gene ontology analysis revealed that most of the altered genes are involved in metabolic process, cellular process and proteolysis. In addition, 486 long intergenic non-coding RNAs were identified altered upon ZIKV infection. Further, we found correlational changes of a number of potential mRNA target genes with that of altered host microRNAs. The outcomes provide a basic understanding of *Ae. aegypti* responses to ZIKV and helps to determine host factors involved in replication or mosquito host anti-viral response against the virus.

Importance

Vector-borne viruses pose great risks on human health. Zika virus has recently emerged as a global threat, rapidly expanding its distribution. Understanding the interactions of the virus with mosquito vectors at the molecular level is vital for devising new approaches in inhibiting virus transmission. In this study, we embarked on analyzing the transcriptional response of *Aedes aegypti* mosquitoes to Zika virus infection. Results showed large changes both in coding and long non-coding RNAs. Analysis of these genes showed similarities with other flaviviruses, including dengue virus, which is transmitted by the same

mosquito vector. The outcomes provide a global picture of changes in the mosquito vector in response to Zika virus infection.

Keywords: *Aedes aegypti*; transcriptome; Zika virus; RNA-Seq; long non-coding RNA; microRNA; odorant binding protein; behavior

Introduction

Flaviviruses are a group of arthropod-borne viruses (arboviruses) that impose huge burdens on global animal and human health. The most known examples of flaviviruses that cause diseases in humans are yellow fever, West Nile, dengue and Zika viruses. Zika virus (ZIKV) has been the most recently emerged mosquito-borne virus. While it was first reported in 1952 from Uganda (1), the virus spread rapidly across the pacific and the Americas in the last 10 years with recent outbreaks in South America (2). The clinical symptoms are variable, ranging from no or mild symptoms to severe neurological disorders such as microcephaly in infants born from infected mothers, or Guillain-Barré syndrome in adults (reviewed in (2, 3)). The virus is mainly transmitted among humans by the bites of mosquito species of the genus *Aedes*, in particular *Aedes aegypti*, when they take a blood meal from infected individuals. The virus first infects the midgut cells of the mosquito and then disseminates into other tissues, finally reaching the salivary glands where they continue to replicate and are eventually transmitted to other human hosts upon subsequent blood feeding events (4).

It is thought that infection by flaviviruses does not cause any detrimental pathological effects on the mosquito vectors (5), reflecting evolutionary adaptations of the viruses with mosquitoes through intricate interactions, which involve optimal utilization of host factors for replication and avoidance of overt antiviral responses. However, a number of studies have shown major transcriptomic changes in the mosquito vectors in response to flavivirus infection. These changes suggest regulation of a wide range of host genes involved in

classical immune pathways, RNA interference, metabolism, energy production and transport (6-13). In addition, mosquito small and long non-coding RNAs have also been shown to change upon flavivirus infection (14, 15).

Recently, we showed that the microRNA (miRNA) profile of *Ae. aegypti* mosquitoes is altered upon ZIKV infection at different time points following infection (16). Here, we describe the transcriptional response of *Ae. aegypti* whole mosquitoes to ZIKV infection at the same time points post-infection. Consistent with previous studies on other arboviruses, we found that the abundance of a large number of genes was altered following ZIKV infection.

Results and Discussion

Ae. aegypti RNA-Seq data analysis

RNA sequencing using Illumina sequencing technology was performed on poly(A)-enriched RNAs extracted from ZIKV-infected and non-infected *Ae. aegypti* mosquitoes at 2, 7, and 14 days post-infection (dpi). Total numbers of clean paired reads varied between 43,486,502 to 60,486,566 reads per library among the 18 sequenced RNA samples. More than 96% of reads mapped to the host genome with around 80% of counted fragments mapped to gene regions and 20% to intergenic areas of the genome (Table S1).

Principal component analysis (PCA) of the RNA-Seq data at each time point distributed all biological replicates of ZIKV-infected and non-infected samples in two distinct groups, although the differences were more subtle at 2 days post-infection, in which one of the ZIKV-infected biological replicates was relatively close to the control group (Fig. 1).

Analysis and comparison of mRNA expression profiles of *Ae. aegypti* mosquitoes at different time points following ZIKV infection revealed that in total 1332 genes had changes of 2-fold or more in either directions (Fig. 2 with details in Table S2). Among the three time points, the highest number of changes occurred at 7 dpi with 944 genes

showing alteration in their transcript levels. The numbers of genes altered at 2 and 14 dpi were very close, 298 and 303, respectively (Fig. 3). These trends were expected as we anticipated to see lower gene expression alteration at 2 dpi and 14 dpi due to low level of infection in the mosquito body at 2 dpi and advanced stages of virus replication at 14 dpi, while at 7 dpi the virus is still at its proliferative stage infecting various tissues of the mosquito. In a previous study that explored the effect of DENV-2 on *Ae. aegypti* transcriptome using RNA-Seq, the number of genes altered at 4 dpi was the highest (151 combining carcass and midgut) as compared to 1 dpi that showed the lowest number of changes (40) followed by 14 dpi (82) (11).

Comparison of the transcriptome profiles showed 18 overlapping genes among the three time points (Fig. 3; listed in Table 1). Twelve of these common genes were depleted and only six were enriched, which were Angiotensin-converting enzyme (AAEL009310), serine-type endopeptidase (AAEL001693), phosphoglycerate dehydrogenase (AAEL005336), cysteine dioxygenase (AAEL007416) and two hypothetical proteins. To validate the analysis of the RNA-Seq data, we used RT-qPCR analysis of nine of the 18 genes. Overall, all genes showed consistency between the two methods in their trends of depletion or enrichment, except for four genes (AAEL013338, AAEL005090, AAEL012339, AAEL013602) the trend was the opposite but this only occurred at 7 dpi (Fig. 4).

Deferentially abundant transcripts and comparisons with other flaviviruses

When concentrating on genes with 10-fold differential expression and statistical significance relative to control mosquitoes, 75, 41 and 16 genes showed changes at 2, 7 and 14 dpi, respectively. After removing hypothetical proteins, those with known functions are listed in Table 2. Interestingly, while the total number of genes showing differential abundance was higher at 7 dpi (Fig. 3), more genes showed 10-fold or greater changes at 2 dpi as compared with 7 dpi (74 versus 41).

At 2 dpi, transcripts of eight genes were enriched with a metalloproteinase (AAEL011539)

showing 56-fold increase in abundance, a serine protease (AAEL013298) increasing 22-fold, and two trypsins (AAEL007601 and AAEL013707) with 19 and 10-fold increases, respectively. We also saw that two phosphatidyl ethanolamine-binding proteins, two cubulin proteins, and a cysteine-rich venom protein were altered at this time point. However most strikingly, we observed suppression of 14 odorant binding proteins at 2 dpi with several of these transcripts being massively reduced (around 800-fold) (Table 2). Furthermore, other odorant binding protein transcripts were enhanced (by 2 fold or greater) at 7 and 14 dpi (Table S2), indicating that ZIKV may have the capacity to alter the behavior of the mosquito, potentially suppressing host-seeking in early stages of the infection and encouraging host-seeking when the mosquito is infectious. Dengue virus is known to alter host-seeking behaviors and feeding efficiency (17, 18), and microarray analysis of mosquitoes with salivary gland infections found several odorant binding protein transcripts that were enhanced in this late stage of infection (14 dpi) (19). Similarly, there is evidence that malaria parasites suppress the host-seeking tendencies of the mosquito early in infection but encourage host-seeking at later stages when the mosquito can transmit the parasite (20-22). The transcription patterns we observed here with ZIKV are consistent with these observations from dengue and malaria infection of mosquitoes but further studies are required to confirm this intriguing finding.

At 7 dpi, 34 genes showed enrichment of 10-fold or more including clip-domain serine proteases, defensins, transferrins, hexamerin, C-type lectin, and serine proteases, which are implicated in immune responses. At this time point, only seven genes were depleted. The number of genes that were differentially expressed by 10-fold or more at 14 dpi was small, with eight genes showing enrichment and eight genes showing depletion. The highest enrichment (212-fold) was steroid receptor RNA activator 1 (AAEL015052), while peritrophin, attacin and superoxide dismutase were among the depleted genes (Table 2).

Previous studies have shown alteration of mRNA transcript levels in *Ae. aegypti*

mosquitoes infected with DENV and a couple of other flaviviruses. Using microarray analysis, Colpitts et al. found that 76 genes showed 5-fold or more changes in DENV-infected mosquitoes over 1, 2 and 7 dpi (13). Their study, which also included response of *Ae. aegypti* to West Nile virus (WNV) and Yellow fever virus (YFV), found commonly 20 and 15 genes were differentially enriched and depleted, respectively, between the three flaviviruses at day 1 post-infection. Histone H3 (AAEL003685) that was enriched at all time points with WNV, YFV and DENV in *Ae. aegypti* (13) was not changed during ZIKV infection, except 2-fold depletion at 7 dpi. Consistent with Colpitts et al, Juvenile hormone-inducible protein (AAEL006607) was induced in ZIKV-infected mosquitoes but only at 7 dpi by 2-fold. A serine protease gene (AAEL006568) depleted by all three flaviviruses was also depleted by ZIKV infection by 2-folds at 2 dpi only. A matrix metalloprotease (AAEL00312) was highly depleted by DENV, WNV and YFV. Two matrix metalloproteases annotated in the new genome assembly (AAEL002672 and AAEL002665) did not change much in ZIKV-infected mosquitoes at 2 and 14 dpi, but were induced by 11.5 and 5.5-folds at 7 dpi. A pupal cuticle protein (AAEL011045) that was significantly depleted in the case of DENV, WNV and YFV, was enriched in ZIKV-infected mosquitoes by about 2-folds at 7 and 14 dpi.

In a follow-up study using the data from the above study (13), Londono-Renteria et al. identified 20 top differentially regulated transcripts in YFV, DENV and WNV infected *Ae. aegypti* mosquitoes (23). Out of these 20 genes, five of them were also found changed in ZIKV-infected mosquitoes in our study. These were the cysteine-rich venom proteins (AAEL005098, AAEL005090, AAEL000379 and AAEL000356) by about 9, 18, 25 and 150-fold depletion at 2 dpi, and an unknown protein (AAEL013122) by 390-fold depletion at 2 dpi. Another study also found a number of cysteine-rich venom proteins altered upon DENV infection of *Ae. aegypti* mosquitoes (11). Cysteine-rich venom proteins are secretory proteins that are mostly found in the fluids of animal venoms acting on ion

channels (24). Londono-Renteria et al. found that among the cysteine-rich venom proteins only AAEL000379 was enriched in DENV-infected mosquitoes and the rest did not change noticeably. Silencing the gene led to increase in replication of DENV (23). Alteration of the cysteine-rich venom proteins commonly found in the case of different flaviviruses indicates their possible importance in replication of these viruses. Further studies are required to determine the role these proteins play in ZIKV-infected mosquitoes specifically.

In another study with DENV-2 and *Ae. aegypti* in which deep sequencing of carcass, midgut and salivary glands were used, transcript levels of infected and non-infected tissues were compared at 1, 4 and 14 dpi, which showed differential abundance of 397 genes (11). We reanalyzed the raw data from the study using the same pipeline as we used for our study. In total, 216 genes were found to be commonly altered between DENV-2 and ZIKV infections (Table S3). At 1 dpi, the highest enrichments of altered genes were related to immunity (holotricin, AAEL017536 and Defensin, AAEL003841), followed by metabolism (fatty acid synthase, AAEL001194 and malic enzyme, AAEL005790) (11). The two immune genes were also enriched in the case of ZIKV infection in this study, but only at 7 dpi (Table S2). The two metabolism related genes changed by about 2.5-fold only at 7 dpi in ZIKV-infected mosquitoes. In the midgut, 10 genes were enriched and 10 were depleted in DENV-infected mosquitoes at 1 dpi as compared to control. Cecropin (AAEL017211) showed the highest depletion in the case of DENV infection, but this gene was not changed in ZIKV-infected mosquitoes in this study. The highest enriched transcripts in DENV-infected mosquito midguts were either associated with oxidoreductase and transport activities or functions unknown (11). A gene associated with transport (AAEL001503) was also changed in ZIKV-infected mosquitoes by about 2.5-fold only at 7 dpi.

At 4 dpi, the transcript levels of 146 genes were altered in DENV-infected *Ae. aegypti* (11). The majority of genes at this time point were depleted in virus-infected samples as

compared to the control. These were mostly associated with immunity. Consistent with the DENV study, attacin, cathepsin, clip-domain serine proteases, a number of C-type lectins, defensin, fibrinogen and holotricin were also altered in ZIKV-infected mosquitoes (Table S2). Redox and metabolism associated genes cytochrome P450, and allantoinase were also among others that showed differential expression in ZIKV and DENV-infected mosquitoes.

At 14 dpi, commonly altered immune genes between DENV and ZIKV infections were C-type lectins and attacin. Enriched in 14 dpi by DENV, Histone H4 (AAEL003673, AAEL003689), Histone H2A (AAEL003669) were depleted by about 2.5-fold at 7 dpi in ZIKV-infected mosquitoes.

A number of immune-related genes were mostly enriched at 7 dpi in ZIKV-infected mosquitoes. Toll was enriched only at 7 dpi by 2-fold. Twelve leucine-rich immune proteins were mostly enriched at 7 dpi by 4-16 folds. Phenoloxidae (AAEL010919), which was not changed upon DENV infection, was depleted by 2-folds at 2 dpi but enriched by 8-9 folds at 7 and 14 dpi in ZIKV-infected mosquitoes. Components of the JAK/STAT pathway, such as Dome and Hop, were not induced in ZIKV-infected mosquitoes. Interestingly, induction of the JAK/STAT pathway specifically in the fat body of *Ae. aegypti* mosquitoes by overexpressing Dome or Hop did not lead to increased resistance to ZIKV infection (25). This result and lack of induction of the pathway in our study suggests that the JAK/STAT pathway may not be involved in ZIKV-mosquito interaction. Further, major genes involved in the RNAi pathway, such as Dicer-1, Dicer-2, or any of the Argonaut genes, also did not change upon ZIKV infection in this study.

Gene Ontology

All the differentially expressed host genes were submitted to Blast2Go for gene ontology (GO) analysis. This analysis identified 126, 68 and 33 GO terms in biological process, molecular function and cellular components, respectively (Table S4). GO analysis revealed

that the majority of differentially expressed genes in biological process category are involved in metabolic process, cellular process and proteolysis (Fig. 5). Binding and catalytic activity are two GO terms which showed significant enrichment among other terms in molecular function (Fig. 5). In *Ae. aegypti*, differentially expressed genes upon infection with DENV, WNV and YFV belonged to various cellular processes, such as metabolic processes, ion binding, peptidase activity and transport (13), which are also among the GO terms identified in differentially abundant transcripts in the ZIKV-infected mosquitoes (Fig. 5).

microRNA target genes

We screened all the differentially expressed mRNAs for the presence of potential microRNA (miRNA) binding sites. We identified 628 highly confident binding sites of 122 *Ae. aegypti* miRNAs in 422 differentially expressed genes (Table S5). Only 77 binding sites are located in the 3'UTRs and 55 in the 5'UTR of these genes.

The output of three predictive tools revealed more than one binding site in 135 differentially expressed genes. Cytochrome P450 (AAEL014019) harbors 10 binding sites in its sequence, Notch (AAEL008069) and Ubiquitin specific protease (AAEL011975) are two other genes with eight binding sites in their sequence. Considering all the examined *Ae. aegypti* miRNAs, miR-34-5p, miR-252-3p, miR-210-5p, miR-309a-3p and miR-2c-3p bind to multiple genes and have more than 20 binding sites. Recently, we identified *Ae. aegypti* miRNAs altered upon ZIKV infection at the same time points that RNA-Seq was conducted (2, 7 and 14 dpi) (16). Comparative analysis and mapping of the altered mRNAs and miRNAs with opposite trends in abundance revealed that 53 of the differentially expressed mRNAs could potentially be regulated by 11 differentially abundant miRNAs (Table S6). However, this is growing evidence that miRNAs could also positively regulate their target genes (26, 27), which are not listed in the table.

Long intergenic non-coding RNAs (lincRNAs) change upon ZIKV infection

lincRNAs are transcripts that are larger than 200 nt but do not code for any proteins, however, they are transcribed the same way as mRNAs (28); i.e. they have a poly-A tail and therefore enriched in transcriptomic data produced following mRNA isolation and sequencing. Similar to small non-coding RNAs, the main function of lincRNAs is regulation of gene expression, involved in various processes such as genomic imprinting and cell differentiation (29), epigenetic and non-epigenetic based gene regulation (30), activation and differentiation of immune cells (31), and relevantly virus-host interactions (32-36).

We recently reported 3,482 putative lincRNAs from *Ae. aegypti* (32). In this study, we found that in total, 486 lincRNAs were differentially expressed in response to ZIKV infection in at least one time point post-infection (fold change, FC > 2 and P-value <0.05). Similar to mRNAs (see Fig. 3), the majority of altered lincRNAs were found at 7 dpi and 56 out of these lincRNAs showed significant alteration at least in two time points (Table S7 and Fig. 6). The Euclidean distance was calculated for each time point based on their lincRNA fold changes. Differentially expressed lincRNAs at 7 dpi (116.83) and 14 dpi (75.30) showed more correlation or similar FC pattern than those of 2 dpi (180.86). Only lincRNAs 656, 1385 and 3105 were differentially expressed and showed the same FC change pattern among the three time points. In our previous study, we also found that the transcript levels of 421 *Ae. aegypti* lincRNAs was altered due to DENV-2 infection. Comparison of those with the ones identified in this study showed that about 80 of them were also differentially expressed in ZIKV-infected samples (Table S7), which could be common lincRNAs involved in flavivirus-mosquito interactions.

Conclusions

Overall, our results showed large changes in the transcriptome of *Ae. aegypti* mosquitoes upon ZIKV infection, both in coding and long non-coding RNAs. The majority of transcriptional changes occurred at 7 dpi, with the genes mostly involved in metabolic process, cellular process and proteolysis. We found some overlaps of transcriptional

alterations in the case of other flavivirus infections in *Ae. aegypti*, but unlike those, immune genes were not altered to the same extent. In regards to lincRNAs, out of 486 lincRNAs changed in ZIKV-infected mosquitoes, 80 of them overlapped with that of DENV-infected mosquitoes indicating possible conserved functions of the lincRNAs in flavivirus-mosquito interactions. A drawback of this study is that we used whole mosquitoes, which means changes at the tissue levels could have been overlooked due to dilution factor by mixing all tissues; however, the outcomes provide a global overview of transcriptional response of *Ae. aegypti* to ZIKV infection, and can be utilized in determining potential pro and anti-viral host factors.

Materials and Methods

Ethics Statement

ZIKV, which was originally isolated from an *Ae. aegypti* mosquito (Chiapas State, Mexico), was obtained from the World Reference Center for Emerging Viruses and Arboviruses at the University of Texas Medical Branch (Galveston, TX, USA). Experimental work with the virus was approved by the University of Texas Medical Branch Institutional Biosafety Committee (Reference number: 2016055).

Mosquito infections with Zika virus

We used excess RNA from samples generated recently to investigate miRNA profiles in ZIKV-infected *Ae. aegypti* mosquitoes (16). Briefly, 4-6 day old female *Ae. aegypti* (Galveston strain) were orally infected with ZIKV (Mex 1-7 strain) at 2 x 10^5 focus forming units (FFU)/ml) in a sheep blood meal (Colorado Serum Company). Infected mosquitoes were collected at 2, 7 and 14 days post-infection (dpi) from which RNA was extracted using the mirVana RNA extraction kit (Life Technologies) applying the protocol for extraction of total RNA. Viral infection in mosquitoes was confirmed by Taqman qPCR on ABI StepOnePlus machine (Applied Biosystems) (16). For all time points, three

284 independent pools were used to create libraries for infected and uninfected samples.
285 Uninfected mosquitoes were fed with ZIKV-free blood, collected at the same time points
286 and processed as above.

287 **Library preparations and sequencing**

288 All samples were quantified using a Qubit fluorescent assay (Thermo Scientific). Total
289 RNA quality was assessed using an RNA 6000 chip on an Agilent 2100 Bioanalyzer
290 (Agilent Technologies).

291 Total RNA (1.0 μg) was poly A+ selected and fragmented using divalent cations and heat
292 (94^0 C, 8 min). The NEBNext Ultra II RNA library kit (New England Biolabs) was used for
293 RNA-Seq library construction. Fragmented poly A+ RNA samples were converted to cDNA
294 by random primed synthesis using ProtoScript II reverse transcriptase (New England
295 Biolabs). After second strand synthesis, the double-stranded DNAs were treated with T4
296 DNA polymerase, 5' phosphorylated and then an adenine residue was added to the 3'
297 ends of the DNA. Adapters were then ligated to the ends of these target template DNAs.
298 After ligation, the template DNAs were amplified (5-9 cycles) using primers specific to each
299 of the non-complimentary sequences in the adapters. This created a library of DNA
300 templates that have non-homologous 5' and 3' ends. A qPCR analysis was performed to
301 determine the template concentration of each library. Reference standards cloned from a
302 HeLa S3 RNA-Seq library were used in the qPCR analysis. Cluster formation was
303 performed using 15.5-17 billion templates per lane using the Illumina cBot v3 system.
304 Sequencing by synthesis, paired end 50 base reads, was performed on an Illumina HiSeq
305 1500 using a protocol recommended by the manufacturer.

306 **RNA-Seq data analysis**

307 The CLC Genomics Workbench version 10.1.1 was used for bioinformatics analyses in
308 this study. RNA-Seq analysis was done by mapping next-generation sequencing reads,

distributing and counting the reads across genes and transcripts. The latest assembly of *Aedes aegypti* genome (GCF_000004015.4) was used as reference. All libraries were trimmed from sequencing primers and adapter sequences. Low quality reads (quality score below 0.05) and reads with more than 2 ambiguous nucleotides were discarded. Clean reads were subjected to RNA-Seq analysis toolbox for mapping reads to the reference genome with mismatch, insertion and deletion cost of 2, 3 and 3, respectively. Mapping was performed with stringent criteria and allowed a length fraction of 0.8 in mapping parameter, which encounter at least 80% of nucleotides in a read must be aligned to the reference genome. The minimum similarity between the aligned region of the read and the reference sequence was set at 80%.

Principal Component Analysis (PCA) graphs were produced for each time point after ZIKV infection between control and infected samples to identify any outlying samples for quality control. The expression levels used as input were normalized log CPM (Count Per Million) values.

The relative expression levels were produced as RPKM (Reads Per Kilobase of exon model per Million mapped reads) values, which take into account the relative size of the transcripts and only uses the mapped-read datasets to determine relative transcript abundance. To explore genes with differential expression profile between two samples, CLC Genomic Workbench uses multi-factorial statistics based on a negative binomial Generalized Linear Model (GLM). Each gene is modeled by a separate GLM and this approach allows us to fit curves to expression values without assuming that the error on the values is normally distributed. TMM (Trimmed mean of M values) normalization method was applied on all data sets to calculate effective library sizes, which were then used as part of the per-sample normalization (37).

The Wald Test was also used to compare each sample against its control group to test whether a given coefficient is non-zero. We considered genes with more than 2-fold

335 change and false discovery rate (FDR) of less than 0.05 as statistically significantly
336 modulated genes.
337 We previously reported 3,482 putative long intergenic non-coding RNAs (lincRNA) from
338 *Ae. aegypti* (32). The expression profile of lincRNAs was also generated for each sample
339 similar to the approach described above.
340 To identify the host transcriptomic response to two different flaviviruses, we compared
341 altered gene profiles in previously published DENV-infected *Ae. aegypti* libraries (11) with
342 our ZIKV infected samples. The relevant RNA-Seq data (SRA058076) were downloaded
343 from NCBI sequence read archive. The libraries were treated in the same way as
344 described above to identify differentially expressed *Ae. aegypti* gene profiles in response
345 to DENV.

346 **Gene Ontology (GO) analysis**

347 All differentially expressed genes were uploaded to Blast2GO server for functional
348 annotation and GO analysis. We used Blast and InterProScan algorithms to reveal the GO
349 terms of differentially expressed sequences. More abundant terms were computed for
350 each category of molecular function, biological process and cellular components.
351 Blast2GO has integrated the FatiGO package for statistical assessment and this package
352 uses the Fisher's Exact Test.

353 **Identification of miRNA target genes**

354 We screened all differentially expressed mRNAs to identify potential miRNA targets among
355 them. If selected mRNAs do not have complete annotation such as clear 5'UTR, ORF and
356 3'UTR, the region before ORF start codon (300 bp) and after stop codon (500 bp) for each
357 mRNA was considered as 5'UTR and 3'UTR, respectively. We used three different
358 algorithms including RNA22 (38), miRanda (39) and RNAhybrid (40) to predict potential
359 miRNA binding sites on genes altered by ZIKV. We previously described this approach
360 and parameters for setting each tool, but to increase the level of confidence, we selected

those binding sites which were predicted by all the three algorithms for further analysis (41).

RT-qPCR analysis of mRNAs

RNA was isolated as described previously (16). RNA from ZIKV positive samples was pooled (N = 5) for time points 2, 7, and 14 dpi and treated with amplification grade DNase I (Invitrogen). Total RNA was reverse transcribed using the amfiRivert cDNA Synthesis Platinum master mix (GenDEPOT, Barker, TX, USA) containing a mixture of oligo $dT_{(18)}$ and random hexamers. Real-time quantification was performed in StepOnePlus instrument (Applied Biosystems, Foster City, California, United States) in 10 µl reaction containing 1:10 diluted cDNA template, 1X PowerUp SYBR Green Master Mix (Applied Biosystems), 1µM each primer. The analysis was performed using ΔΔCt (Livak) method (42). Three independent biological replicates were conducted and all PCRs were performed in duplicates. The ribosomal protein S7 gene (43) was used for normalization of cDNA templates. Primer sequences are listed in Table S8.

Accession number

The accession number for the raw and trimmed sequencing data reported here is GEO: GSEXXXXX.

Acknowledgements

This project was supported by a NIH grant (R21AI124452) and a University of Texas Rising Star award to GLH, and an Australian Research Council (DP150101782) and an Australian Infectious Disease Research Centre grant to SA. GLH is additionally supported by the Western Gulf Center of Excellence for Vector-borne Diseases (CDC grant CK17-005). MAS was supported by a NIH T32 fellowship.

Author contributions: conceptualization, S.A., and G.L.H; Investigation: K.E., S.H., M.A.S., S.G.W., and T.G.W.; Data curation: K.E.; Formal analysis: K.E., and S.A.; Writing-original

draft: K.E., and S.A.; Writing-review & editing: S.A., and G.L.H.; Supervision: S.A., and G.L.H.

References

1. Dick GW, Kitchen SF, Haddow AJ. 1952. Zika virus. I. Isolations and serological specificity. Trans R Soc Trop Med Hyg 46:509-520.
2. Song BH, Yun SI, Woolley M, Lee YM. 2017. Zika virus: History, epidemiology, transmission, and clinical presentation. J Neuroimmunol 308:50-64.
3. Miner JJ, Diamond MS. 2017. Zika virus pathogenesis and tissue tropism. Cell Host Microbe 21:134-142.
4. Weaver SC, Costa F, Garcia-Blanco MA, Ko AI, Ribeiro GS, Saade G, Shi PY, Vasilakis N. 2016. Zika virus: History, emergence, biology, and prospects for control. Antiviral Res 130:69-80.
5. Blair CD, Olson KE. 2014. Mosquito immune responses to arbovirus infections. Curr Opin Insect Sci 3:22-29.
6. Xi Z, Ramirez JL, Dimopoulos G. 2008. The *Aedes aegypti* Toll pathway controls dengue virus infection. PLoS Pathog 4:e1000098.
7. Sanchez-Vargas I, Scott J, Poole-Smith B, Franz A, Barbosa-Solomieu V, Wilusz J, Olson K, Blair C. 2009. Dengue virus type 2 infections of *Aedes aegypti* are modulated by the mosquito's RNA interference pathway. PLoS Pathog 5:e1000299.
8. Sim S, Dimopoulos G. 2010. Dengue virus inhibits immune responses in *Aedes aegypti* cells. PLoS One 5:e10678.
9. Tchankouo-Nguetcheu S, Khun H, Pincet L, Roux P, Bahut M, Huerre M, Guette C, Choumet V. 2010. Differential protein modulation in midguts of *Aedes aegypti* infected with chikungunya and dengue 2 viruses. PLoS One 5.
10. Behura SK, Gomez-Machorro C, Harker BW, deBruyn B, Lovin DD, Hemme RR, Mori A, Romero-Severson J, Severson DW. 2011. Global cross-talk of genes of the mosquito *Aedes aegypti* in response to dengue virus infection. PLoS Negl Trop Dis 5:e1385.
11. Bonizzoni M, Dunn W, Campbell C, Olson K, Marinotti O, James A. 2012. Complex modulation of the *Aedes aegypti* transcriptome in response to dengue virus infection. PLoS One 7:e50512.
12. Chauhan C, Behura SK, Debruyn B, Lovin DD, Harker BW, Gomez-Machorro C, Mori A, Romero-Severson J, Severson DW. 2012. Comparative expression profiles of midgut genes in dengue virus refractory and susceptible *Aedes aegypti* across critical period for virus infection. PLoS One 7:e47350.
13. Colpitts TM, Cox J, Vanlandingham DL, Feitosa FM, Cheng G, Kurscheid S, Wang P, Krishnan MN, Higgs S, Fikrig E. 2011. Alterations in the *Aedes aegypti* transcriptome during infection with West Nile, Dengue and Yellow fever viruses. PLoS Pathog 7:e1002189.
14. Campbell CL, Black WCt, Hess AM, Foy BD. 2008. Comparative genomics of small RNA regulatory pathway components in vector mosquitoes. BMC Genomics 9:425.
15. Etebari K, Osei-Amo S, Blomberg S, Asgari S. 2015. Dengue virus infection alters post-transcriptional modification of microRNAs in the mosquito vector *Aedes aegypti*. Sci Rep 5:15968.
16. Saldaña MA, Etebari K, Hart CE, Widen SG, Wood TG, Thangamani S, Asgari S, Hughes GL. 2017. Zika virus alters the microRNA expression profile and elicits an RNAi response in *Aedes aegypti* mosquitoes. PLoS Neg Trop Dis 11:e0005760.

17. Maciel-de-Freitas R, Sylvestre G, Gandini M, Koella JC. 2013. The influence of dengue virus serotype-2 infection on *Aedes aegypti* (Diptera: Culicidae) motivation and avidity to blood feed. PLoS One 8:e65252.
18. Sylvestre G, Gandini M, Maciel-de-Freitas R. 2013. Age-dependent effects of oral infection with dengue virus on *Aedes aegypti* (Diptera: Culicidae) feeding behavior, survival, oviposition success and fecundity. PLoS One 8:e59933.
19. Sim S, Ramirez JL, Dimopoulos G. 2012. Dengue virus infection of the *Aedes aegypti* salivary gland and chemosensory apparatus induces genes that modulate infection and blood-feeding behavior. PLoS Pathog 8:e1002631.
20. Murdock CC, Luckhart S, Cator LJ. 2017. Immunity, host physiology, and behaviour in infected vectors. Curr Opin Insect Sci 20:28-33.
21. Cator LJ, George J, Blanford S, Murdock CC, Baker TC, Read AF, Thomas MB. 2013. 'Manipulation' without the parasite: altered feeding behaviour of mosquitoes is not dependent on infection with malaria parasites. Proc Biol Sci 280:20130711.
22. Cator LJ, Lynch PA, Read AF, Thomas MB. 2012. Do malaria parasites manipulate mosquitoes? Trends Parasitol 28:466-70.
23. Londono-Renteria B, Troupin A, Conway MJ, Vesely D, Ledizet M, Roundy CM, Cloherty E, Jameson S, Vanlandingham D, Higgs S, Fikrig E, Colpitts TM. 2015. Dengue virus infection of *Aedes aegypti* requires a putative cysteine rich venom protein. PLoS Pathog 11:e1005202.
24. Gibbs GM, O'Bryan MK. 2007. Cysteine rich secretory proteins in reproduction and venom. Soc Reprod Fertil Suppl 65:261-267.
25. Jupatanakul N, Sim S, Anglero-Rodriguez YI, Souza-Neto J, Das S, Poti KE, Rossi SL, Bergren N, Vasilakis N, Dimopoulos G. 2017. Engineered *Aedes aegypti* JAK/STAT pathway-mediated immunity to dengue virus. PLoS Negl Trop Dis 11:e0005187.
26. Vasudevan S. 2012. Posttranscriptional upregulation by microRNAs. RNA 3:311-330.
27. Vasudevan S, Tong Y, Steitz JA. 2007. Switching from repression to activation: microRNAs can up-regulate translation. Science 318:1931-1934.
28. Clark MB, Mattick JS. 2011. Long noncoding RNAs in cell biology. Semin Cell Dev Biol 22:366-376.
29. Bonasio R, Shiekhattar R. 2014. Regulation of transcription by long noncoding RNAs. Annu Rev Genet 48:433-455.
30. Mercer TR, Dinger ME, Mattick JS. 2009. Long non-coding RNAs: insights into functions. Nat Rev Genet 10:155-159.
31. Fitzgerald KA, Caffrey DR. 2014. Long noncoding RNAs in innate and adaptive immunity. Curr Opin Immunol 26:140-146.
32. Etebari K, Asad S, Zhang G, Asgari S. 2016. Identification of *Aedes aegypti* long intergenic non-coding RNAs and their association with *Wolbachia* and dengue virus infection. PLoS Negl Trop Dis 10:e0005069.
33. Lakhotia SC. 2012. Long non-coding RNAs coordinate cellular responses to stress. RNA 3:779-796.
34. Mizutani R, Wakamatsu A, Tanaka N, Yoshida H, Tochigi N, Suzuki Y, Oonishi T, Tani H, Tano K, Ijiri K, Isogai T, Akimitsu N. 2012. Identification and characterization of novel genotoxic stress-inducible nuclear long noncoding RNAs in mammalian cells. PLoS One 7:e34949.
35. Tani H, Onuma Y, Ito Y, Torimura M. 2014. Long non-coding RNAs as surrogate indicators for chemical stress responses in human-induced pluripotent stem cells. PLoS One 9:e106282.

36. Winterling C, Koch M, Koeppel M, Garcia-Alcalde F, Karlas A, Meyer TF. 2014. Evidence for a crucial role of a host non-coding RNA in influenza A virus replication. RNA Biol 11:66-75.
37. Robinson M, Oshlack A. 2010. A scaling normalization method for differential expression analysis of RNA-seq data. Genome Biol 11:R25.
38. Miranda KC, Huynh T, Tay Y, Ang Y-S, Tam W-L, Thomson AM, Lim B, Rigoutsos I. 2006. A pattern-based method for the identification of microRNA binding sites and their corresponding heteroduplexes. Cell 126:1203-1217.
39. Enright AJ, John B, Gaul U, Tuschl T, Sander C, Marks DS. 2003. MicroRNA targets in *Drosophila*. Genome Biol 5:R1.
40. Krueger J, Rehmsmeier M. 2006. RNAhybrid: microRNA target prediction easy, fast and flexible. Nucleic Acids Res 34:W451-W454.
41. Etebari K, Asgari S. 2016. Revised annotation of *Plutella xylostella* microRNAs and their genome-wide target identification. Insect Mol Biol 25:788-799.
42. Liu Y, Zhou Y, Wu J, Zheng P, Li Y, Zheng X, Puthiyakunnon S, Tu Z, Chen X. 2015. The expression profile of *Aedes albopictus* miRNAs is altered by dengue virus serotype-2 infection. Cell Biosci 5:16.
43. Isoe J, Collins J, Badgandi H, Day WA, Miesfeld RL. 2011. Defects in coatomer protein I (COPI) transport cause blood feeding-induced mortality in Yellow Fever mosquitoes. Proc Natl Acad Sci USA 108:E211-7.

Figure legends

Figure 1. The principal component analysis of the effect of ZIKV infection on *Ae. aegypti* transcriptome at three different time points post-infection. The normalized log CPM (Count Per Million) used as expression value in this analysis.

Figure 2. Volcano plot analysis. Red circles indicate differentially expressed mRNAs in response to ZIKV infection (Fold change > 2 and FDR < 0.05).

Figure 3. Venn diagram representing the number of differentially expressed coding genes at three different time points post ZIKV infection. Profound alteration in gene expression was observed at 7 dpi and more common differentially expressed genes were found between day 7 and 14 samples.

Figure 4. Validation of RNA-Seq data analysis by RT-qPCR. Overall, all genes showed consistency between the two methods in their trends of depletion or enrichment, except for four genes (AAEL013338, AAEL005090, AAEL012339, AAEL013602) the trend was the opposite only at 7 dpi.

Figure 5. GO term enrichment analysis of differentially expressed genes in response to ZIKV infection in three categories of biological process, molecular function, and cellular component.

Figure 6. Venn diagram representing the number of differentially expressed lincRNAs at three different time points post ZIKV infection (FC > 2 and P-value <0.05). The majority of altered lincRNAs were found at 7 dpi and 56 out of these lincRNAs showed significant alteration at least at two time points.

Table 1. List of *Ae. aegypti* differentially expressed genes common to all the three time points post ZIKV infection.

Gene ID	Gene Description	Fold change (Day 2)	FDR p-value	Fold change (Day 7)	FDR p-value	Fold change (Day 14)	FDR p-value
AAEL009310	Angiotensin-converting enzyme	5.41	3.66E-08	3.18	4.61E-04	2.65	4.81E-03
AAEL001693	Serine-type endopeptidase	4.08	8.02E-05	2.33	4.74E-03	2.46	3.81E-03
AAEL005336	D-3-phosphoglycerate dehydrogenase	2.06	0.02	2.81	3.00E-09	2.15	1.66E-03
AAEL010153	Protein bicaudal C	-2.59	9.34E-03	-2.81	0	-3.08	8.26E-13
AAEL003688	Conserved hypothetical protein	-2.21	3.40E-03	-2.13	5.98E-12	-2.23	3.00E-08
AAEL005501	B-box type zinc finger protein ncl-1	-2.87	4.86E-05	-2.13	5.55E-10	-2.6	1.72E-06
AAEL017329	B-box type zinc finger protein ncl-1	-2.52	6.34E-04	-2.14	8.32E-08	-2.44	9.77E-09
AAEL005850	Hormone receptor-like in 4 (nuclear receptor)	-2.57	8.90E-04	-2.75	3.66E-13	-3.06	1.23E-08
AAEL007416	Cysteine dioxygenase	3.12	7.28E-03	2.37	0.02	4.52	5.85E-08
AAEL010086	DNA replication licensing factor MCM4	-2.2	5.94E-03	-2.15	2.33E-10	-2.4	1.90E-07
AAEL010228	Conserved hypothetical protein	2.54	0.03	6.45	1.29E-09	3.12	3.10E-06
AAEL010644	Ribonucleoside-diphosphate reductase large chain	-2.3	0.03	-2.62	0	-2.28	5.52E-07
AAEL011811	DNA replication licensing factor MCM3	-2.03	8.63E-03	-2.37	0	-2.21	1.90E-07
AAEL012339	Cdk1	-2	4.40E-03	-2.58	1.05E-07	-2.82	5.07E-08
AAEL013338	Lethal (2) essential for life protein, l2efl	-2.78	5.28E-05	-3.3	0	-2.38	8.43E-08
AAEL013577	Conserved hypothetical protein	3.7	5.81E-04	2.81	0.02	7.57	2.13E-06
AAEL013602	Laminin gamma-3 chain	-2.31	6.85E-03	-2.03	2.80E-03	-2.29	4.66E-04
AAEL003797	Hypothetical protein	-2.82	4.43E-03	-3.12	9.61E-11	-2.18	2.47E-03

Table 2. List of *Ae. aegypti* differentially expressed genes with more than 10-fold change at each time point (in bold) post ZIKV infection.

			Fold change		
Name	**Gene ID**	**Description**	**Day 2**	**Day 7**	**Day 14**
AAEL011539	5574950	metalloproteinase, putative	**56.2**	-1.1	3.31
AAEL013298	5577578	serine protease, putative	**22.08**	1.86	4.74
AAEL007601	5569396	trypsin 5G1-like	**18.98**	3.46	3.06
AAEL013707	5578506	trypsin 5G1-like	**10.07**	6.24	1.81
AAEL011260	5574623	protein D3	**-10.95**	3.1	-0.18
AAEL011954	5575620	elongation of very long chain fatty acids protein 7	**-11.96**	1.56	1.14
AAEL014312	5564093	cubilin homolog	**-12.1**	8.42	1.87
AAEL010965	5574152	cubilin homolog	**-12.49**	1.4	-1.61
AAEL010139	5572918	putative defense protein 1	**-14.85**	34.42	0.9
AAEL003094	5577074	glycoprotein, putative	**-16.59**	6.43	-1.29
AAEL011491	5574891	general odorant-binding protein 67	**-17.05**	-2.93	0.46
AAEL001487	5570904	general odorant-binding protein 45-like	**-17.49**	-	2.66
AAEL004947	5565723	elongation of very long chain fatty acids protein 4	**-18.74**	-2.25	5.11E-03
AAEL005090	5565985	cysteine#ich venom protein, putative	**-18.75**	3.74	-
AAEL010875	5574034	general odorant-binding protein 45-like	**-20.22**	-	-
AAEL007096	5568731	major royal jelly protein 3	**-21.97**	1.01	0.67
AAEL010848	5574004	major royal jelly protein 5	**-23.73**	1.45	-0.67
AAEL010872	5574030	general odorant-binding protein 45-like	**-27.81**	-8.89	0.38
AAEL011808	5575404	glucose dehydrogenase [FAD, quinone	**-29.51**	-1.01	3.95E-03
AAEL006398	5567938	OBP32: odorant binding protein OBP32	**-31.43**	1.71	-
AAEL006393	5567943	OBP28: odorant binding protein OBP28	**-35.93**	-6.24	-
AAEL005925	5567269	geranylgeranyl pyrophosphate synthase	**-38.51**	3.74	2.96E-03
AAEL006396	5567937	OBP31: odorant binding protein OBP31	**-56.46**	-3.6	-1.31
AAEL003511	5578352	general odorant-binding protein 45-like	**-59.39**	-1.75	0.79
AAEL015262	5566792	phosphatidylethanolamine-binding protein, putative	**-59.59**	1.4	0.56
AAEL000796	5566894	general odorant-binding protein 45-like	**-302.47**	3.74	2.66
AAEL015052	5566038	steroid receptor RNA activator 1	**-358.45**	3.11	7.73
AAEL000827	5566899	general odorant-binding protein 45-like	**-362.89**	-1.75	-
AAEL000846	5566895	general odorant-binding protein 45-like	**-397.26**	2.42	0.51
AAEL000833	5566896	general odorant-binding protein 45-like	**-739.97**	2.42	1.27
AAEL000835	5566905	general odorant-binding protein 45-like	**-811.93**	-	-0.78
AAEL000837	5566897	general odorant-binding protein 45-like	**-883.73**	-1.01	2.67
AAEL000701	5565919	39S ribosomal protein L4, mitochondrial	1.25	**438.21**	-
AAEL015019	5565969	protein artichoke	-1.43	**42.54**	1.31
DEFD	5579095	defensin-A-like	-8.11	**31.28**	-4.25
AAEL014386	5564283	serine protease easter	-2.06	**30.31**	2.23
DEFA_AEDAE	5579099	defensin-A	-7.35	**21.99**	-4.45
AAEL015430	5579444	serine protease, putative	-1.19	**21.79**	-1.05
AAEL015639	5579270	transferrin	-3.55	**19.09**	-1.67
AAEL014005	5579131	clip-domain serine protease, putative	-2.03	**17.69**	1.47
CTLMA15	5563672	C-type lectin 37Da	-1.1	**16.19**	3.91

TRY5_AEDAE	5578510	trypsin 5G1	-1.15	**15.52**	2.13
DEFC_AEDAE	5579094	defensin-C	-8.23	**14.5**	-5.59
AAEL013640	5578322	lung carbonyl reductase	3.51	**13.7**	1.49
AAEL010429	5573346	protein G12	5.92	**13.51**	25.07
AAEL002726	5575756	37 kDa salivary gland allergen Aed a 2-like	1.09	**12.19**	1.63
AAEL015458	5579417	transferrin	-9.02	**11.93**	-1.19
AAEL013542	5578161	elongation of very long chain fatty acids	-1.65	**11.85**	2.91
AAEL002672	5575549	matrix metalloproteinase-19	-1.25	**11.49**	1.36
AAEL013990	5579047	hexamerin-1.1	-1.16	**10.97**	1.96
AAEL005787	5567041	serine protease easter	-1.05	**10.3**	1.72
AAEL015628	5579281	glycine dehydrogenase	2.92	**10.07**	1.84
AAEL004134	5564162	lupus la ribonucleoprotein	2.24	**-69.95**	-2.86
AAEL003946	5563782	28S ribosomal protein S33, mitochondrial	-2.19	**-101.56**	1.57
AAEL009497	5572080	probable phosphomannomutase	-1.25	**-676.56**	-3.51
AAEL015052	5566038	steroid receptor RNA activator 1	-358.45	3.11	**212.47**
AAEL010429	5573346	protein G12	5.92	13.51	**25.07**
AAEL009435	5571953	adhesion regulating molecule 1	-1.34	-1.21	**13.51**
AAEL002613	5575308	peritrophin-48	3.23	-3.98	**11.35**
ATT	5578028	attacin-B	4.4	-1.42	**-10.49**
AAEL007040	5568687	protein lozenge, transcript variant X3	-1.83	45.7	**-12.57**
AAEL011550	5574942	seminal metalloprotease 1	-1.93	1.71	**-22.18**
CUSOD3_a	5573744	superoxide dismutase [Cu-Zn	1.03	1.18	**-39.11**

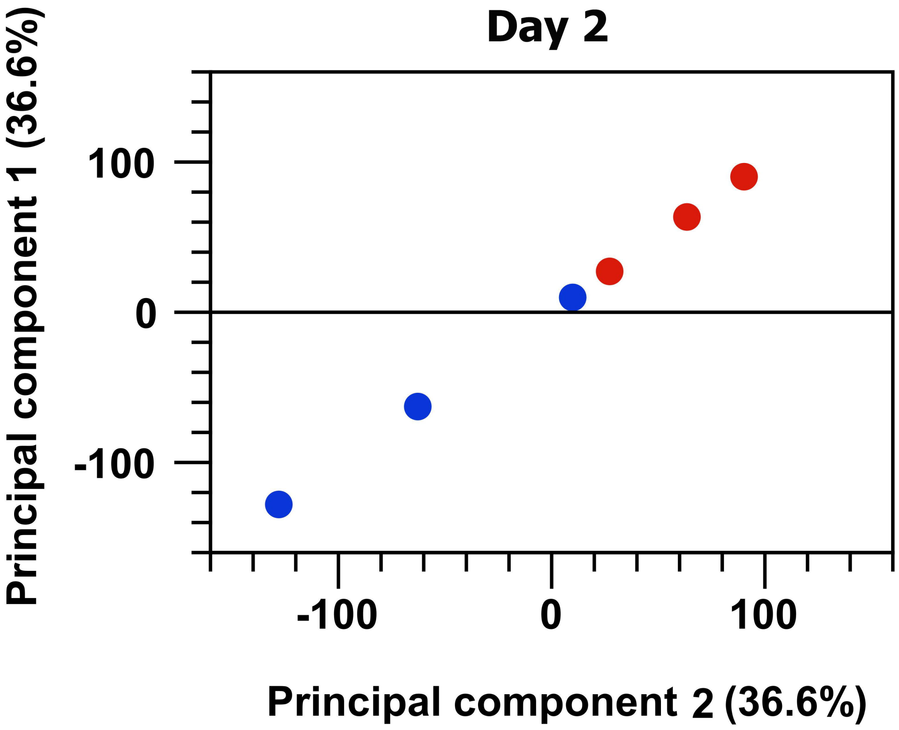

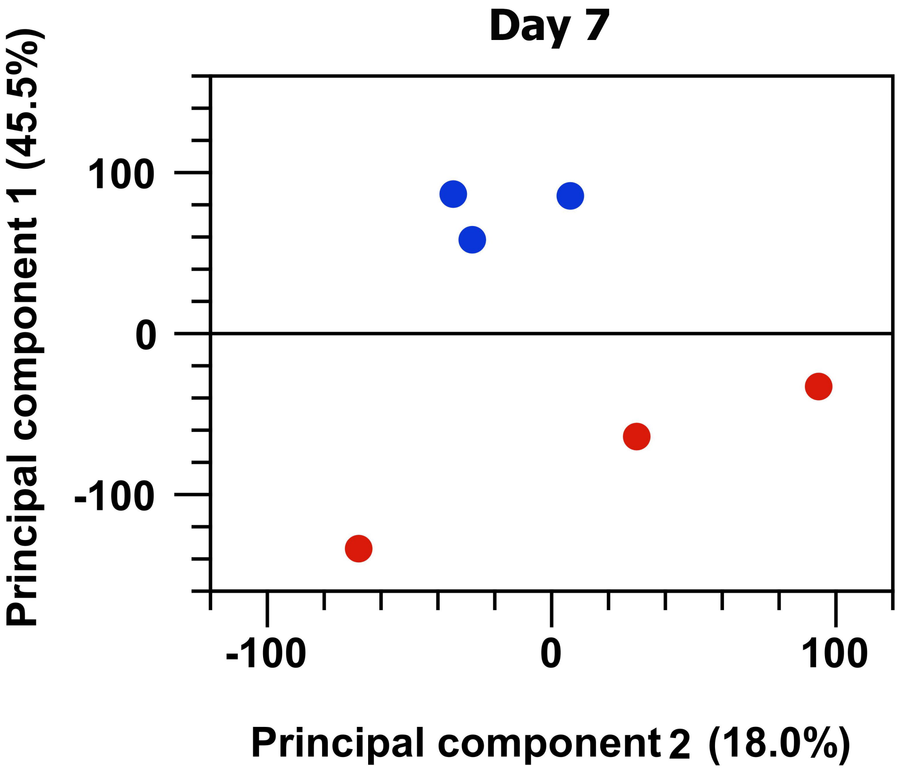

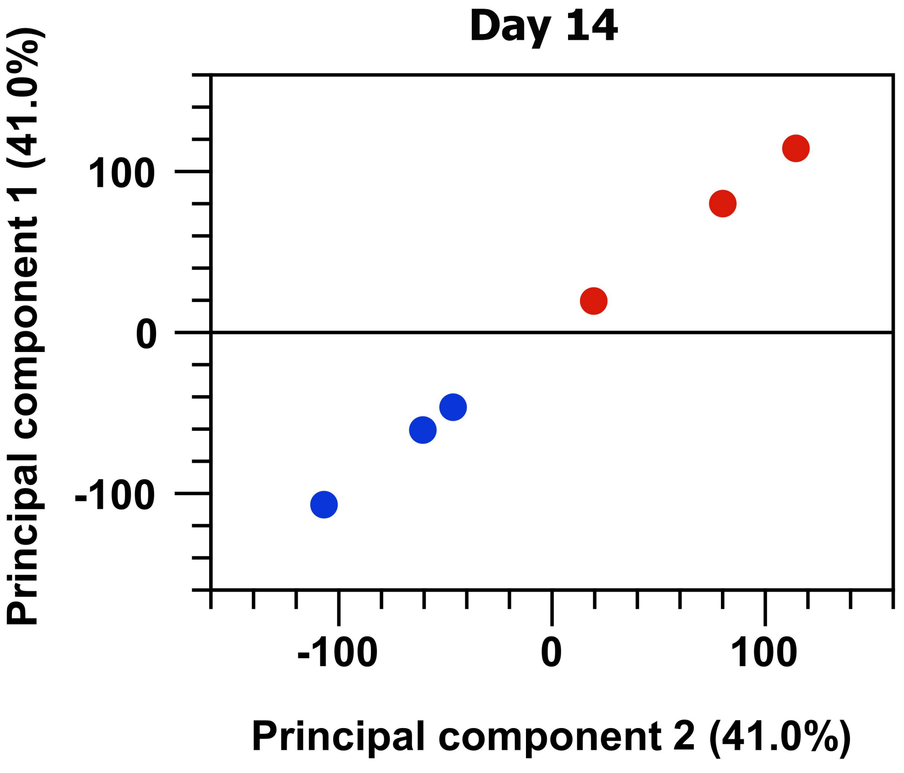

Control ZIKV Infected

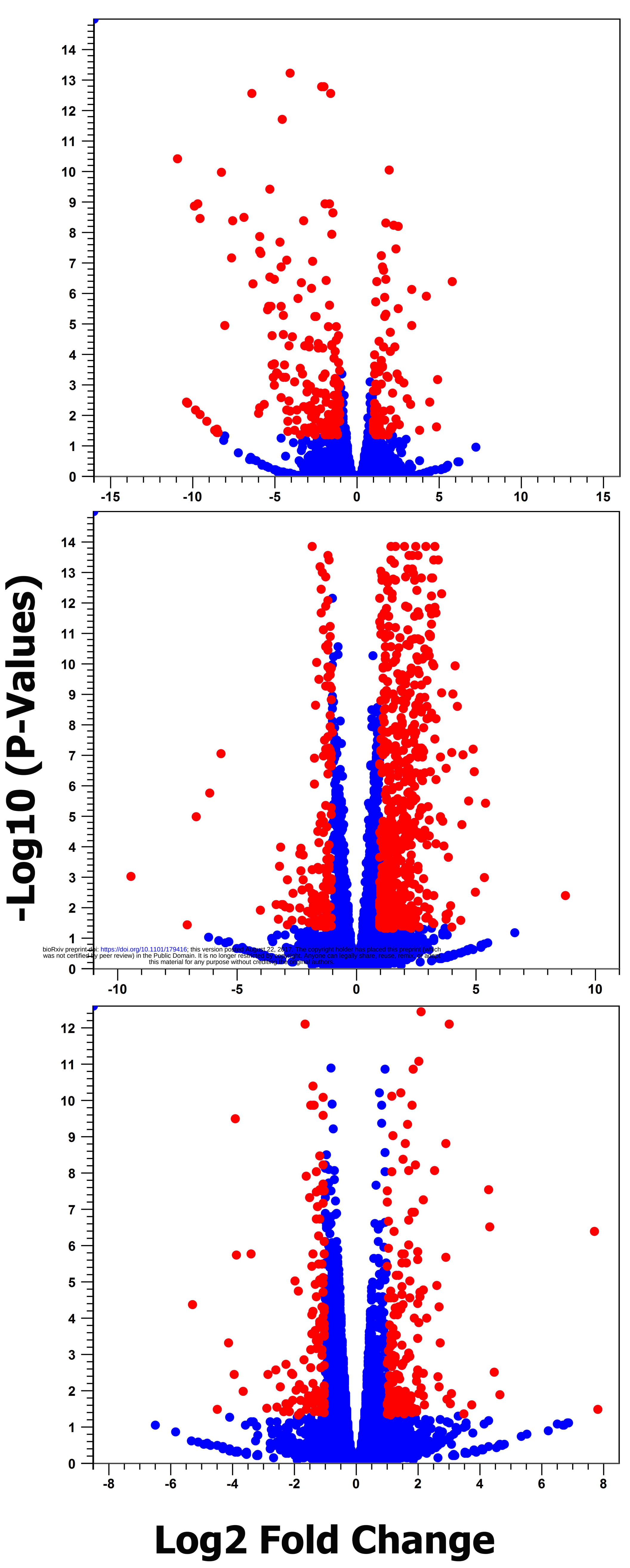

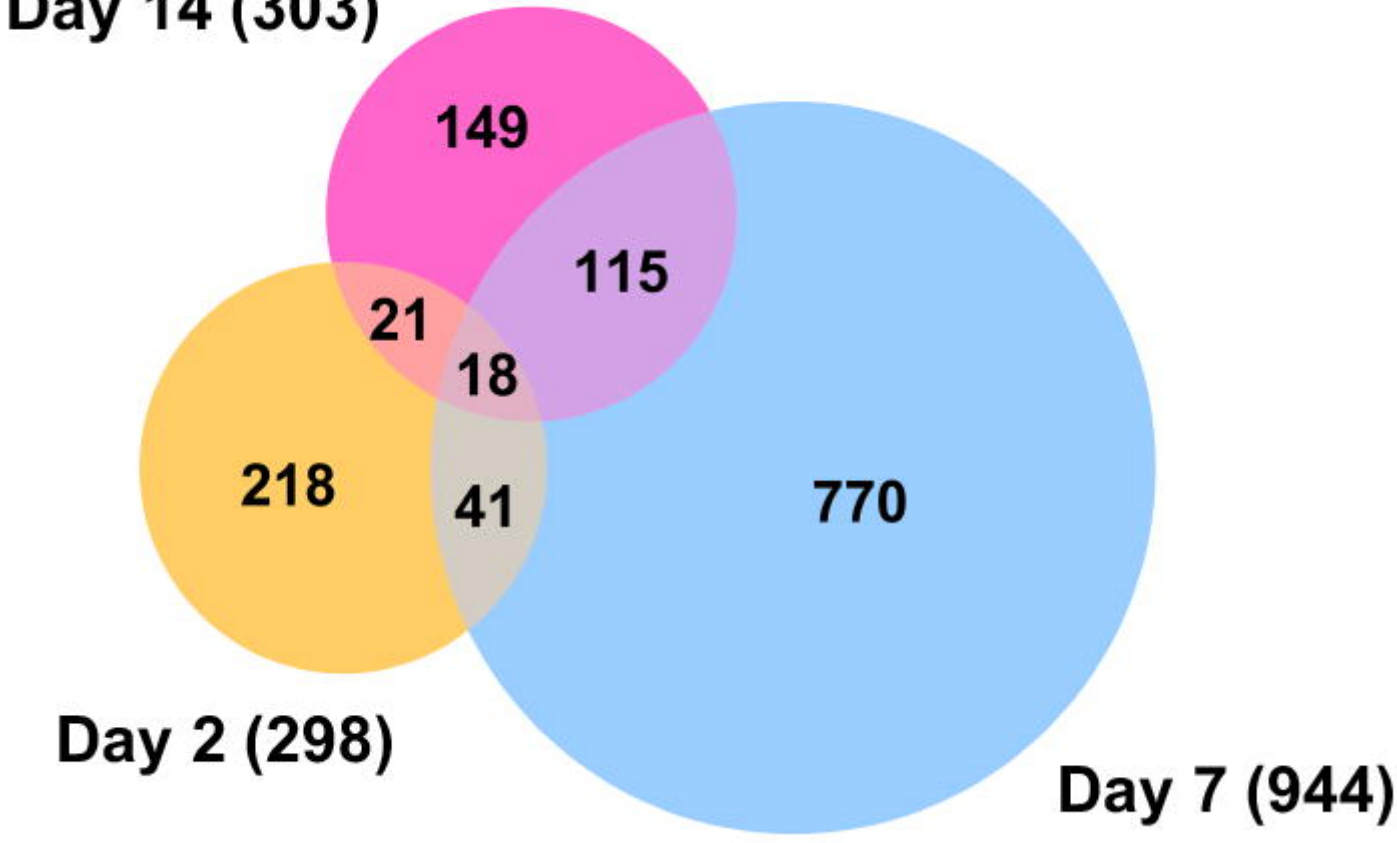
Day 14 (303)
149
115
21
18
218
41
770
Day 2 (298)
Day 7 (944)

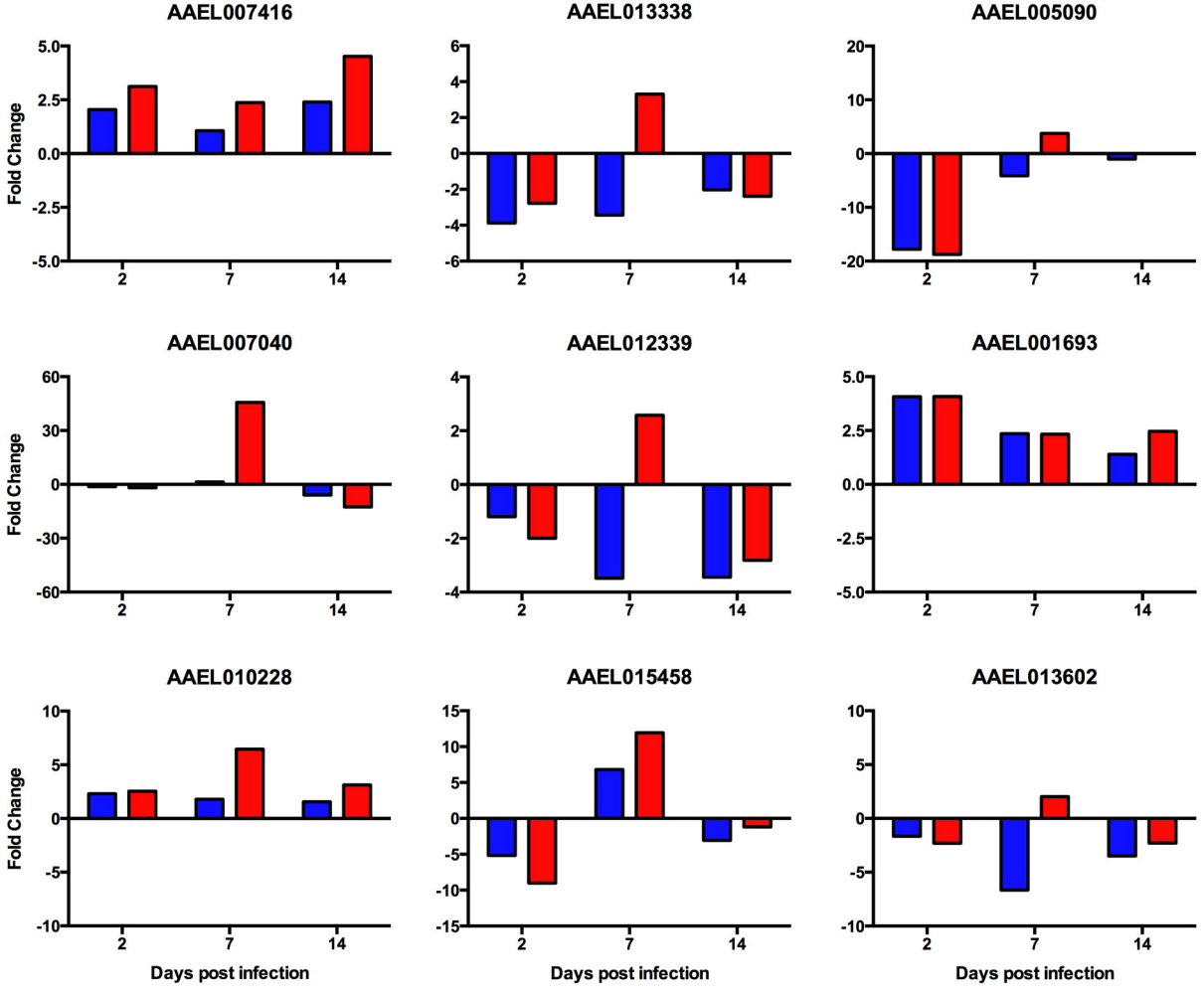
AAEL007416
AAEL013338
AAEL005090
AAEL007040
AAEL012339
AAEL001693
AAEL010228
AAEL015458
AAEL013602
Fold Change
Days post infection
2
7
14
qPCR fold change
Transcriptomics

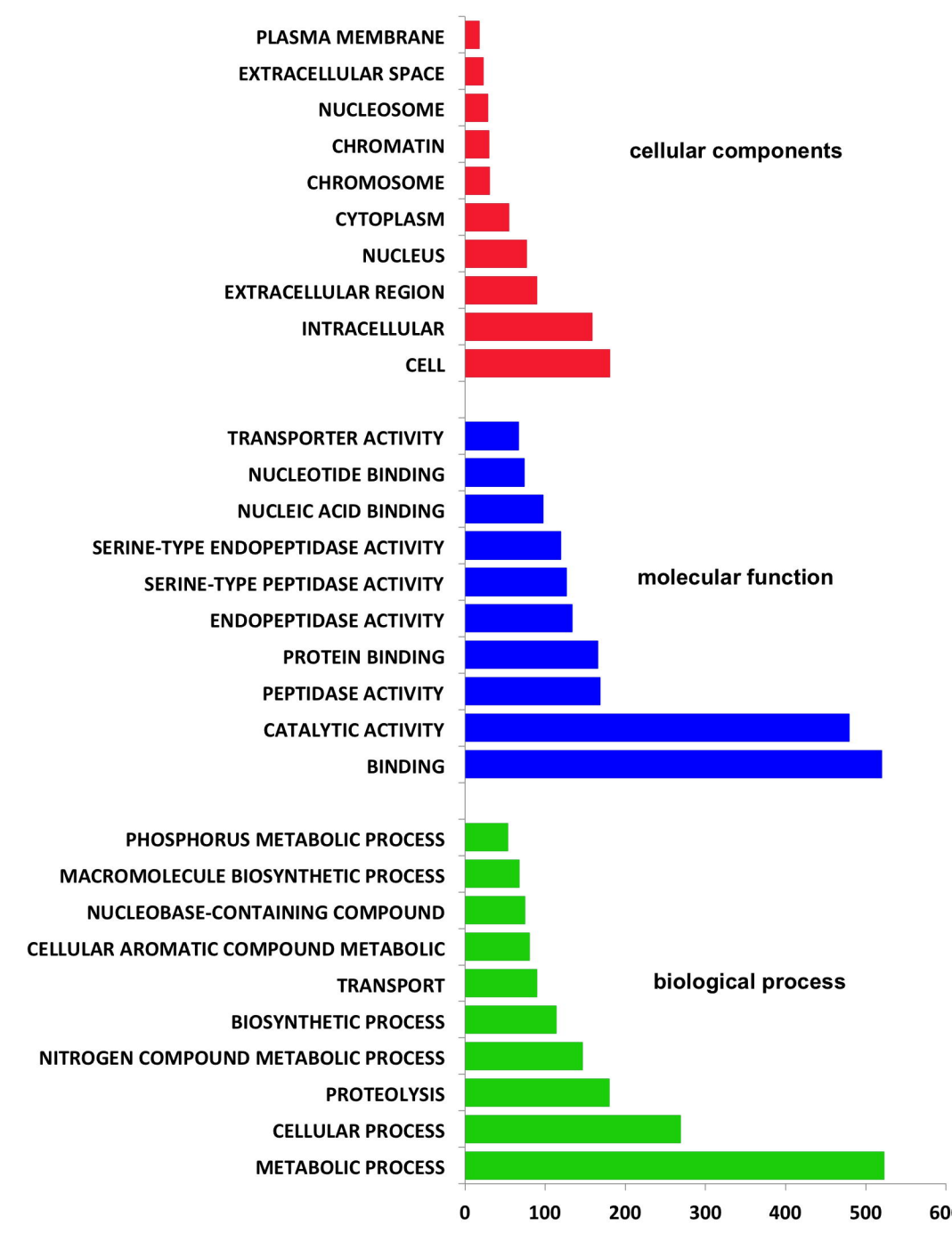
PLASMA MEMBRANE
EXTRACELLULAR SPACE
NUCLEOSOME
CHROMATIN
CHROMOSOME
CYTOPLASM
NUCLEUS
EXTRACELLULAR REGION
INTRACELLULAR
CELL
cellular components
TRANSPORTER ACTIVITY
NUCLEOTIDE BINDING
NUCLEIC ACID BINDING
SERINE-TYPE ENDOPEPTIDASE ACTIVITY
SERINE-TYPE PEPTIDASE ACTIVITY
ENDOPEPTIDASE ACTIVITY
PROTEIN BINDING
PEPTIDASE ACTIVITY
CATALYTIC ACTIVITY
BINDING
molecular function
PHOSPHORUS METABOLIC PROCESS
MACROMOLECULE BIOSYNTHETIC PROCESS
NUCLEOBASE-CONTAINING COMPOUND
CELLULAR AROMATIC COMPOUND METABOLIC
TRANSPORT
BIOSYNTHETIC PROCESS
NITROGEN COMPOUND METABOLIC PROCESS
PROTEOLYSIS
CELLULAR PROCESS
METABOLIC PROCESS
biological process
0
100
200
300
400
500
600

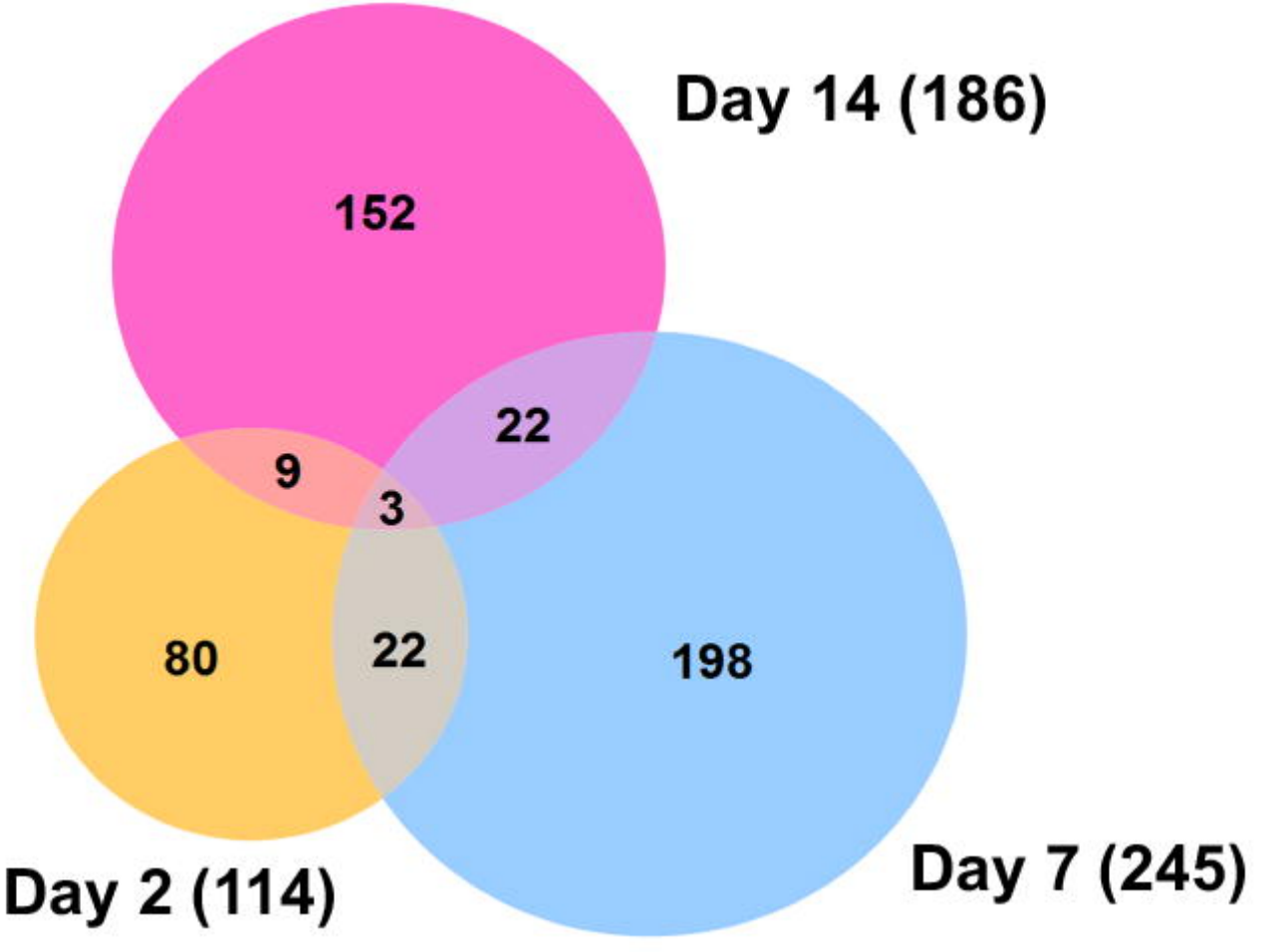
Day 14 (186)
152
22
9
3
80
22
198
Day 2 (114)
Day 7 (245)